Mind the time : 24-hour rhythms in drug exposure and effect

Kervezee, L.

CHAPTER

Diurnal variation in the pharmacokinetics and brain distribution of morphine

7

Laura Kervezee[1,2]; Robin Hartman[2]; Dirk-Jan van den Berg[2]; Johanna H. Meijer[1,*]; Elizabeth C.M. de Lange[2,*]

[1]Laboratory for Neurophysiology, Department of Molecular Cell Biology, Leiden University Medical Center, Leiden, the Netherlands;
[2]Division of Pharmacology, Leiden Academic Center for Drug Research, Leiden University, Leiden, the Netherlands
*These authors share senior authorship

Submitted

ABSTRACT

The pharmacokinetics and pharmacodynamics of drugs are influenced by daily fluctuations in physiological processes. The aim of this study was to determine the effect of dosing time on the pharmacokinetics and brain distribution of morphine. To this end, 4 mg/kg morphine was administered intravenously to male Wistar rats that were either pre-treated with a vehicle solution or tariquidar and probenecid to inhibit processes involved in the active transport of morphine. Non-linear mixed effects modelling was used to describe the concentration-time profiles of morphine and its metabolite M3G in plasma and brain tissue. We find that the efflux of morphine from brain tissue back into the circulation is characterized by a 24-hour rhythm with the lowest efflux during the two light-dark phase transitions with a difference between peak and trough of 20%. The active processes involved in the clearance of morphine and its metabolite M3G from plasma also show 24-hour variation with the highest value in the middle of the dark phase being 54% higher than the lowest value at the start of the light phase. As a result of these fluctuations in pharmacokinetic parameters, the concentrations of morphine in the brain and of M3G in plasma depend on the time of day. Hence, time of day presents a considerable source of variation in the pharmacokinetics of morphine, which could be used to optimize the dosing strategy of morphine.

INTRODUCTION

Morphine is the most widely used opioid for the treatment of moderate to severe pain, despite the many side-effects associated with its use. Therefore, establishing a dosing regimen that results in adequate analgesia and minimal adverse side-effects is crucial, but remains a challenge due to the high degree of intra- and interindividual variability associated with the pharmacokinetics and pharmacodynamics of this drug (Sverrisdóttir et al., 2015). Time of day presents a considerable source of variation in the pharmacokinetics and pharmacodynamics of a wide variety of drugs due to daily rhythms in physiological processes (Dallmann et al., 2014).

There are several indications that time of day influences morphine's effect. For example, it has been shown that the requirement of self-administered morphine fluctuates over the 24-hour period in patients with post-operative pain (Junker and Wirz, 2010; Potts et al., 2011). Additionally, in mice, the analgesic effect of morphine depends on the time of administration: while most studies found that the analgesic effect of morphine is highest during the dark period (Bornschein et al., 1977; Cui et al., 2005; Lutsch and Morris, 1971; Morris and Lutsch, 1967; Yoshida et al., 2003, 2005), some reports found that the analgesic effect of morphine either follows the 24-hour pattern in baseline pain sensitivity (Kavaliers and Hirst, 1983; Oliverio et al., 1982) or is highest during the light period (Güney et al., 1998; Rasmussen and Farr, 2003). However, the physiological mechanisms that underlie these variations in morphine-induced analgesia are unknown.

To gain a more structured overview of the effect of dosing time on the therapeutic effect of morphine, it is essential to first determine 24-hour variation in the pharmacokinetics and in the brain distribution of morphine. Although the effect of dosing time on the exposure to morphine has previously received some attention (Dohoo, 1997; Gourlay et al., 1995), these studies neither determined the 24-hour variation in the different pharmacokinetic parameters of morphine, nor did they address the 24-hour variation in its distribution to the brain, morphine's main site of action.

The concentration of morphine in blood and subsequently in the central nervous system depends on several processes. For example, morphine is primarily metabolized by UDP glucuronosyl transferase (UGT) 2B7 in the liver (De Gregori et al., 2011; Somogyi et al., 2007), the expression of which is regulated by the molecular clock and shows 24-hour variation (Dallmann et al., 2014; Zhang et al., 2009). Additionally, morphine brain distribution is affected by efflux transport proteins such as P-glycoprotein and probenecid-sensitive transporters such as multidrug-resistance proteins (mrps) (Sverrisdóttir et al., 2015; Thompson et al., 2000; Tunblad et al., 2003; Xie et al., 1999). P-glycoprotein mediated transport in the brain depends on the time of drug administration (Kervezee et al., 2014).

To determine 24-hour variation in the pharmacokinetic parameters of morphine, we used a study design in which morphine is intravenously administered to rats at six time-points during the 24-hour period combined with a pharmacokinetic modelling approach. Results from this study enhance our understanding of the processes that underlie the

observed time-of-day dependent analgesic effect of morphine.

METHODS & MATERIALS

Animals

Male Wister WU rats (Charles River, the Netherlands) were housed in groups for at least twelve days under standard environmental conditions (humidity 60%, ambient temperature 21oC) with food (Laboratory chow, Hope Farms, Woerden, The Netherlands) and water ad libitum. After surgery, animals were kept individually until the end of the experiment under otherwise similar conditions. Half of the animals were kept in a light-dark cycle with lights on at 8:00 and lights off at 20:00; the other half was kept under a reversed schedule (8:00 lights off, 20:00 lights on). The weight of the animals was monitored daily. The animal procedures were performed in accordance with the Dutch law on animal experimentation and were approved by the Animal Ethics Committee of the Leiden University (protocol number DEC14041).

Study design

Cannulation of the femoral artery and vein was performed as described previously (Westerhout et al., 2012). Anesthesia was induced and maintained by respectively 5% and 1-2% isoflurane throughout the surgical procedures. Experiments were conducted seven days after surgery and started at one of six different time points (t =0 at either Zeitgeber time (ZT) 0, 4, 8, 12, 16 or 20, with ZT12 defined as the moment that lights are turned off). Experiments that took place during the dark phase were conducted under dim red light. At t= -25 min, tariquidar (15mg/kg; XR9576 from Avant pharmaceuticals, London, UK, in 5% glucose) or vehicle (5% glucose) was administered for 10 minutes, followed by administration of probenecid (150mg/kg; Sigma-Aldrich, Zwijndrecht, the Netherlands, in 5% $NaHCO_3$) or vehicle (5% $NaHCO_3$) for 10 minutes. Half of the animals received a combination of tariquidar and probenecid (inhibitor-treated group), the other half received the two vehicle solutions (vehicle-treated group). At t=0, morphine HCl (4mg/kg; Pharmachemie BV, Haarlem, the Netherlands in saline) was administered for 10 minutes. All drugs were administered intravenously using a syringe pump (Pump 22 Multiple Syringe Pump, Harvard Apparatus, Holliston, MA, USA). Blood samples (150 µL) were drawn at t=-5, 10, 20, 30, 45, 60, 90 and 120 min as well as at t = 180 and/or 240 min, depending on when the experiment was terminated. Blood was collected in heparinized Eppendorf cups and centrifuged for 10 min at 5000 rpm (Eppendorf Microcentrifuge Model 5415D) at 4°C to separate plasma from other blood constituents. Plasma samples were stored on ice until the end of the experiment and subsequently at -20°C until further analysis.

At either t=120, 180 or 240 min, animals were euthanized by an overdose of Nembutal, transcardially perfused and decapitated. Brain tissue was removed, immediately placed on ice and subsequently stored at -80°C until further analysis.

SPE-LC-MS/MS analysis

Morphine and morphine-3-glucoronide (M3G) were measured in plasma and brain tissue using liquid chromatography tandem mass spectrometry (LC-MS/MS). The SPE-LC-MS system consisted of a Finnigan Surveyor MS pump, a Finnigan TSQ Quantum Ultra triple quadrupole system (Thermo Fisher Scientific, Breda, The Netherlands), a SPE cartridge holder and a HySphere Resin GP Cartridge (Spark-Holland, Emmen, The Netherlands) and a Shimadzu Nexera UHPLC system. A Vision HT column 150×2.1mm, 5µm, Basic (Grace Altech, Breda, The Netherlands) with a column filter of 2µm (Phenomenex, Utrecht, The Netherlands) was used for all chromatographic separations. The sheath gas flow was set to 40 and the auxiliary gas flow was set to 55 (Arbitrary units). The capillary temperature was 275 0C and the spray voltage was 3500V.

For the analysis of plasma samples, 20µL of internal standard (1000ng/mL mix of deuterated morphine and M3G), 20µL milli-Q H2O were added to an aliquot of 20µL sample. Protein precipitation was done by adding 1mL of acetonitrile (Biosolve BV, Valkenswaard, the Netherlands) and centrifuging for 10 minutes at 20,000xg (Eppendorf Microcentrifuge Model 5415D, Eppendorf AG, Hamburg, Germany). The supernatant was evaporated by a CentriVap Vacuum Concentration System (Labconco, Kansas City, MO, USA).

Brain tissue samples were homogenized using a Bullet Blender 5 (Next Advance Inc, Averill Park, NY, USA) as described previously [23]. An aliquot of 600µL brain homogenate, 100µL internal standard (500ng/mL morphine-D3 and M3G-D3) and 100µL MQ H2O were mixed before addition of 5mL acetonitrile. After centrifugation at 3800xg, samples were evaporated by a vortex evaporator (Labconco, Kansas City, MO, USA).

Pellets from either plasma and brain tissue samples were subsequently dissolved by sonification after adding 40µL (to plasma samples) or 100µL (to brain samples) 10mM ammonium acetate pH10. After centrifugation for 10min at 20,000xg, samples were transferred to a glass HPLC vial. The calibration curve ranged from 5 to10000 ng/mL for plasma measurements, and from 5 to 2000 ng/mL for brain tissue measurements. 10µL was injected onto the LCMS system.

After injection of the sample, the SPE column was flushed with 1mL 10 mM ammonium acetate pH 10 (mobile phase A) for 1 minute to remove the salts and other interferences. After the loading step, the SPE was switched in line with the LC column and the compounds were eluted onto the LC column. Flushing of the SPE column was performed under acidic conditions by 3 mL of 90 % acetonitrile with 0.1 % formic acid at a flow rate of 1mL/min. The SPE column was re-equilibrated before the next injection with mobile phase A at a flow of 0.5mL/min for 4 min. Each SPE column was used for a maximum of 100 injections. The compounds were separated by the LC system with an increasing percentage of acetonitrile (from 3 to 97% in 4 min) with 0.1% formic acid at a flow of 200µL/min. The calibration curves of morphine and M3G were constructed by linear regression (weighing factor 1/Y) using LCQuan software.

The inter-assay accuracy for morphine and M3G in plasma and brain tissue was between 91 and 111%, and the intra-assay variability was below 15%. The lower limit of quantification

was 5ng/mL for both morphine and M3G in plasma and brain tissue. Concentrations of M3G in brain tissue were consistently below LLOQ and were therefore not included in further data processing.

Data processing

Samples below LLOQ (<1%) were marked in the data set but were retained, as described previously (Keizer et al., 2015). Concentrations (ng/mL) were converted to nanamol/mL using the molecular weight of morphine.HCl (321.8g/mol) and M3G (free base) (461.47g/mol). Based on protein binding values of morphine in rats that have been reported previously (Bickel et al., 1996; Boström et al., 2008; Letrent et al., 1999; Stain-Texier et al., 1999; Tunblad et al., 2004), an unbound fraction of 70% was used. The degree of plasma protein binding of M3G is very low (unbound fraction of 93% (Bickel et al., 1996)) and was not taken into account in further analysis.

Population pharmacokinetic model development

A population pharmacokinetic model was developed to describe the concentration-time profiles of morphine and M3G in plasma and in morphine brain tissue using nonlinear mixed effects modelling (NONMEM 7.3; Beal et al., 2009), in combination with Pirana (v2.8.2), PsN (v3.7.6), Xpose (v4) and R (v3.1.2) to facilitate evaluation and graphical representation of the models (Keizer et al., 2013).

To compare the fit of nested models, the likelihood ratio test was used, under the assumption that the difference in -2 log-likelihood is χ^2 distributed with degrees of freedom (d.f.) determined by the number of additional parameters in the more complex model. Hence, a decrease in Objective Function Value (OFV) of at least 3.84 points (p-value <0.05) with one additional parameter was considered to provide a significantly better fit of the data compared to its parent model. The fit of non-nested models were compared using the Akaike Information Criterion (AIC) (Mould and Upton, 2013).The first-order method with conditional estimation and interaction (FOCEI) and the ADVAN6 subroutine with user-specified differential equations were used throughout model development. Model selection was based on OFV, precision and plausibility of parameter estimates, graphical evaluation of the goodness of fit and visual predictive checks (VPC).

Interanimal variability was described using Equation 1:

$$P_i = P * e^{\eta i} \qquad \text{Equation 1}$$

Where P_i is the individual parameter estimate of the i^{th} animal, P is the typical parameter estimate in the population and η_i is the interanimal variability for the i^{th} animal. Additive, proportional and combined error models were considered to describe the residual variability (Mould and Upton, 2013).

Pre-treatment with probenecid and tariquidar was assumed to inhibit all active transport processes. Therefore, this effect was assessed on clearance parameters as follows:

$$P = \theta_{passive} + \theta_{active} * (1 - TRT) \qquad \text{Equation 2}$$

where $\theta_{passive}$ is the passive component of the clearance parameter, θ_{active} is the active component of the clearance parameter and TRT is the treatment group (0 for vehicle-treated animals; 1 for inhibitor-treated animals). The effect of the inhibitors on other (non-clearance) parameters was assessed as follows:

$$P = \theta * \theta_{INH}^{TRT} \quad \text{Equation 3}$$

where θ_{INH} is the fractional change in parameter θ in the presence of inhibitor treatment.

A sequential approach was used to develop the population PK model. In the first step, a PK model was developed for morphine and M3G concentrations in plasma. Different structural models were considered (different number of peripheral compartments, linear or Michaelis-Menten clearance). Interanimal variability was assessed on the parameters and the effect of active transport inhibition treatment were considered using a forward inclusion approach. The volume of the M3G compartment was set equal to the volume of the central morphine compartment to yield a structurally identifiable model.

In the second step, the morphine concentrations in brain tissue were added to the data set and the PK model was extended to describe the concentration profile in brain tissue. Because one brain tissue concentration was available per animal, interanimal variability was not investigated on these parameters.

Lastly, the effect of time of day on the pharmacokinetic parameters was assessed. As an exploratory approach, the distribution of conditional weighted residuals with interaction (CWRESI) over time was investigated per treatment-group. Subsequently, it was investigated whether the model fit could be improved by describing one or more parameters by a sinusoidal function with a principal period of 24-hour and one or more harmonic terms (Equation 4).

$$P = \theta_{Mesor} + \Sigma_{(n=1)}^{N} [\theta_{Amplitude,n} * \cos(2\pi * n * (t - \theta_{\varphi,n}) / 24] \quad \text{Equation 4}$$

In this equation, θ_{Mesor} represents the rhythm-adjusted mean value of the parameter, N is the total number of harmonics included in the model, $\theta_{Amplitude,n}$ is the amplitude of the n^{th} harmonic, $\theta_{\varphi,n}$ is the acrophase (time of peak in minutes after onset of light period) of the n^{th} harmonic and t is the time with t=0 defined as the onset of the light period. The number of harmonic terms included in the model was determined by the criteria for statistical significance described above.

Simulations

Simulations to assess the effect of 24-hour variation in the pharmacokinetic parameters on the concentration-time profiles of morphine and M3G in plasma and brain were performed using the package deSolve (v1.11) in R. Two dosing regimens were simulated: 1) a single 10min. intravenous infusion of 4 mg/kg morphine to a rat of 250g with dosing at 0, 4, 8, 12, 16 and 20 hours after onset of the light period and 2) a continuous infusion of 0.5mg/kg/h to a rat of 250g for 24 hours starting at 4 and 16 hours after the onset of the light period.

RESULTS

Morphine and M3G pharmacokinetics in plasma

Data from three animals were missing due to complications during surgery and data from four animals were missing due to difficulties with the cannulas during the experiment, so data from 89 animals (mean weight ± standard deviation: 269 ± 29g) were available for pharmacometric analysis. Table 1 shows the number of animals per treatment group. Morphine and M3G concentrations in plasma in vehicle-treated animals and in inhibitor-treated animals at each of the six dosing times is shown in upper and middle panels of Figure 1.

Table 1 Number of animals per treatment group

Dosing time	No. of vehicle-treated animals	No. of inhibitor-treated animals
0	7	5
4	8	7
8	8	8
12	8	7
16	8	7
20	8	8
TOTAL	47	42

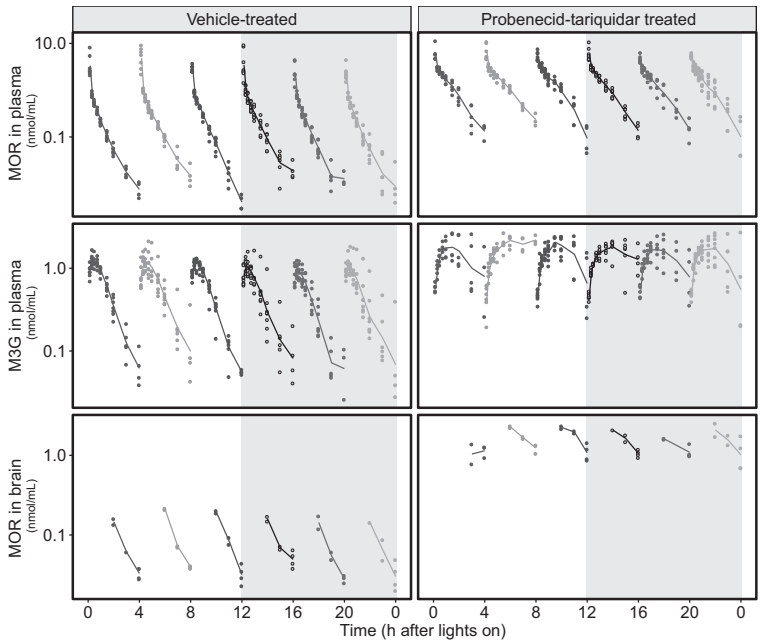

Figure 1 Concentration profiles of morphine (MOR) in plasma (upper panels), M3G in plasma (middle panels) and MOR in brain tissue (lower panels) in vehicle-treated (left) and inhibitor-treated animals (right) after different dosing times.

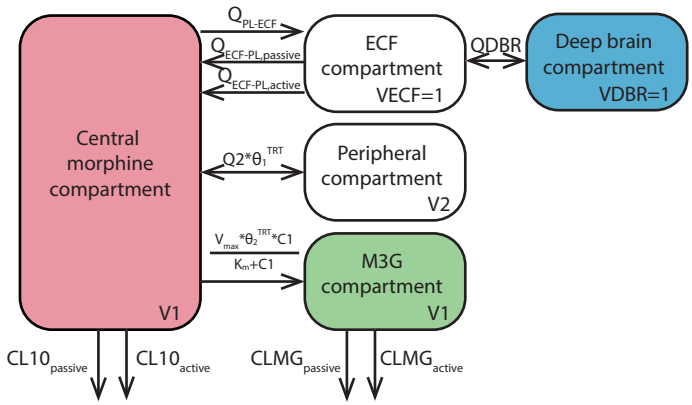

Figure 2 Structure of the final combined plasma-brain model. Colored compartments indicated the site of sampling (red: morphine concentrations in plasma; green: M3G concentrations in plasma; blue: morphine concentrations in brain tissue).

The concentration-time profiles of morphine were initially described by a model consisting of a central compartment, one peripheral compartment and linear clearance from the body. It was attempted to include a second peripheral morphine compartment, but the parameter estimates were very sensitive to the initial values that were provided, so this was not included in the model. To account for the difference in morphine pharmacokinetics between vehicle-treated animals and inhibitor-treated animals, the clearance of morphine from the body (CL_{10}) was split into an active and a passive component as described in Equation 2, resulting in a significant improvement of the model fit (ΔOFV -208, $p<0.01$, 1 d.f.) and reducing the interanimal variability on CL_{10} from 123% to 23%.

The conversion of morphine to M3G was at first described as a linear process, but it was found that it showed concentration-dependent saturation that could be described by Michaelis-Menten kinetics (ΔOFV -402, $p<0.01$, 1 d.f.). Subsequent incorporation of interanimal variability and the effect of inhibitor treatment resulted in a model with interanimal variability included on CL_{10}, the clearance of M3G from plasma (CL_{M3G}), intercompartmental clearance (Q_2) and the maximum conversion rate of morphine to M3G (V_{max}).

Morphine pharmacokinetics in brain tissue

Morphine concentrations in brain tissue in vehicle-treated animals and inhibitor-treated animals at each of the six dosing times are shown in the lower panels of Figure 1. The plasma model was extended to describe these concentration-time profiles. The base model, consisting of one brain compartment and inter-compartmental clearance (Q_{BR}) to describe the transport to and from plasma, described the brain concentrations poorly and showed high residual unexplained variability (128%). In subsequent modelling steps, it was found that a model that described the brain concentrations as deep brain concentrations that was indirectly linked to the central plasma compartment by a transit compartment referred to as the extra-cellular fluid (ECF) compartment, known as an important compartment

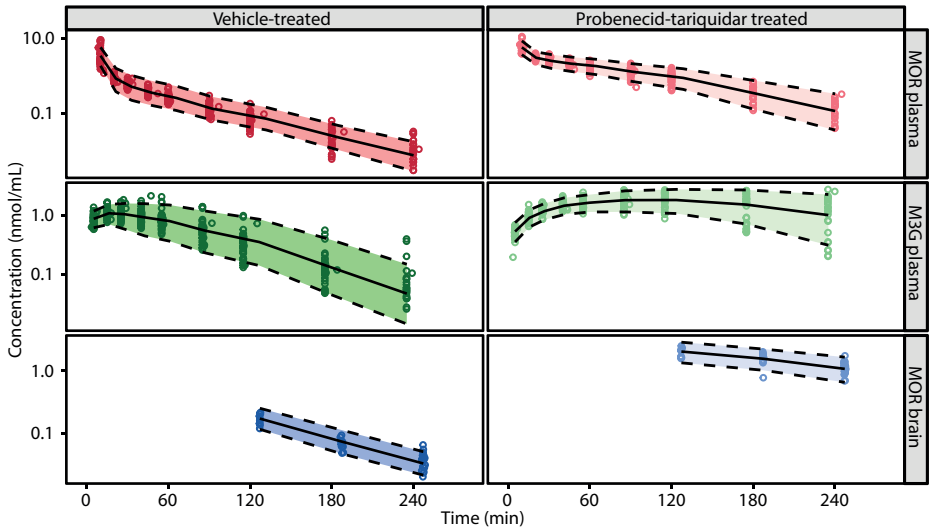

Figure 3 Visual predictive check (VPC) stratified by treatment group. Dots: observed data; solid line: median of the predicted concentrations; shaded areas enclosed by dashed lines: 90% prediction intervals of the simulated data.

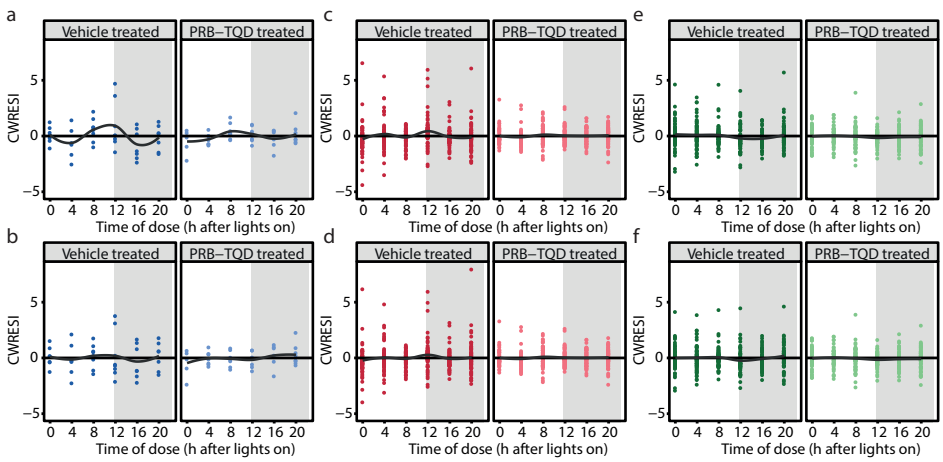

Figure 4 Distribution of CWRESI vs time of dose in vehicle-treated (dark symbols) and probenecid (PRB) – tariquidar (TQD) treated (light symbols) animals. **(a, c, e)** CWRESI distribution in the model without cosine functions of morphine concentrations in brain (a) and in plasma (c) and of M3G concentrations in plasma (e). **(b)** CWRESI distribution in the model with a 24+12-hour cosine included on $Q_{ECF\text{-}PL}$ of morphine concentrations in brain. **(d, f)** CWRESI distribution in the model with a 24+12-hour cosine function included on $CL_{10,active}$ and $CL_{M3G,\ active}$ of morphine concentrations in plasma (d) and of M3G concentrations in plasma (f).

for morphine distribution into the brain (Bouw et al., 2000), could best describe the brain concentrations data. In the final brain model, drug transport between the deep brain compartment and the ECF compartment were described by a single clearance parameter and the flow between the ECF compartment and the plasma compartment by an influx parameter ($Q_{PL\text{-}ECF}$) and an efflux parameter that was split into a passive ($Q_{ECF\text{-}PL,passive}$) and an active ($Q_{ECF\text{-}PL,active}$) component (Figure 2).

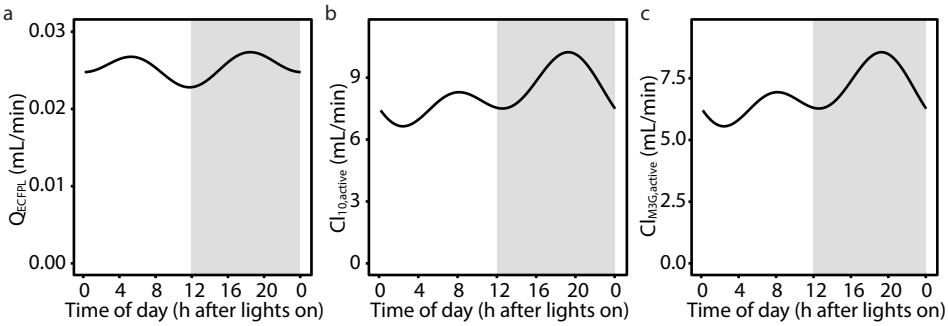

Figure 5 Shape of the cosine functions included on Q_{ECF-PL} (a), $CL_{10,active}$ (b) and $CL_{M3G,active}$ (c).

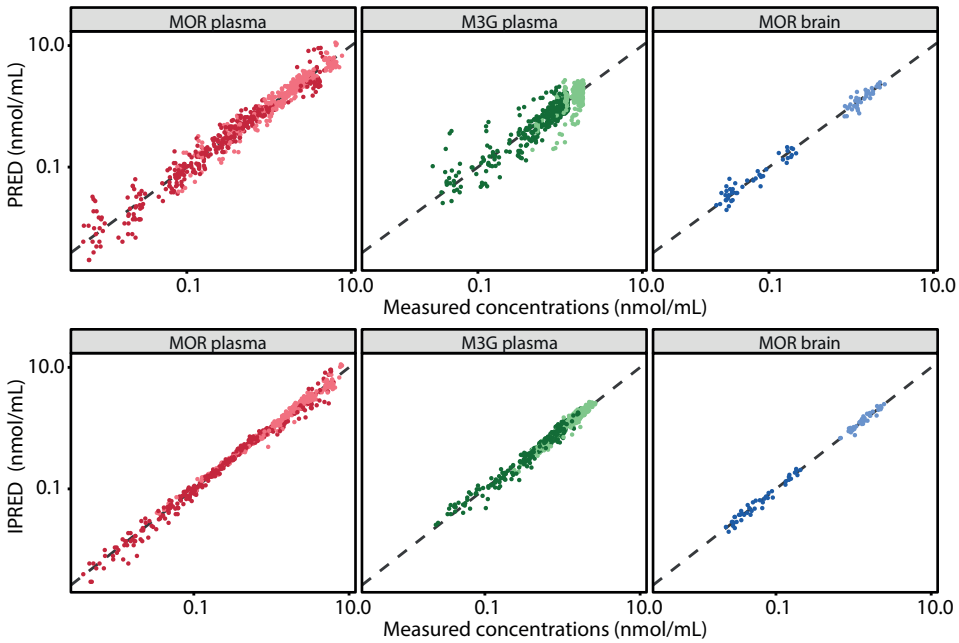

Figure 6 Measured versus population predicted (PRED; upper panels) and individual predicted (IPRED; lower panels) concentrations of morphine (MOR) in plasma (left, red), M3G in plasma (middle, green) and MOR in brain tissue (right, blue) of the final model. Dark coloured symbols represent vehicle-treated animals; light coloured symbols represent inhibitor-treated animals. Dotted line: line of unity.

The volumes of the ECF and deep brain compartment were fixed to 1, because these values could not be estimated with sufficient precision. This model described the central trend and the variability in the brain concentrations well (Figure 3). The parameter estimates of the final combined plasma and brain model are shown in Supplemental Table 1. Of note, the residual unexplained variability of the brain concentrations was reduced from 128% to 13%.

Twenty-four hour variation in morphine pharmacokinetics

The distribution of CWRESI of the morphine concentrations in brain of both vehicle and inhibitor-treated animals showed clear time-of-day dependent bias with peaks around

the light-dark transitions (Figure 4A). Inclusion of a two-harmonic cosine function with a 24-hour and 12-hour component on the efflux of morphine from the ECF compartment to plasma (Q_{ECF-PL}) significantly improved the fit of the model (ΔOFV -16, p<0.005, 4 d.f.). This cosine function adequately removed this bias (Figure 4B) and provided a better fit compared to implementation of a two-harmonic cosine function on the influx parameter (Q_{PL-ECF}) (AIC = -2.7). Moreover, residual unexplained variability of the brain concentrations was reduced from 13.1% to 11.9%. The 24-hour and 12-hour components of this cosine function had a peak at 22.8 hours and 5.9 hours after lights on and relative amplitudes of 4.1% and 6.3%, respectively (Figure 5A).

The CWRESI of morphine and M3G in plasma did not reveal a time-of-day dependent bias (Figure 4C and E). Nevertheless, it was found that inclusion of the same two-harmonic cosine with a 24-hour and 12-hour component on $CL_{M3G,active}$ and $CL_{10,active}$ significantly improved the fit of the model (ΔOFV -28, p<0.005, 4 d.f.). Inclusion of this cosine minimally affected the distribution of CWRESI over time-of-day (Figure 4D and F). The 24-hour and 12-hour components of this cosine function had a peak at 18 hours and 7.6 hours after lights on and relative amplitudes of 13% and 12.5%, respectively (Figure 5B and C).

In the final model (Run8202), the cosine function on Q_{ECF-PL} was combined with the cosine functions on $CL_{M3G,active}$ and $CL_{10,active.}$ This model described the observed concentrations well (Figure 6). Parameter estimates from this model and from a bootstrap (500 runs) are shown in Table 2.

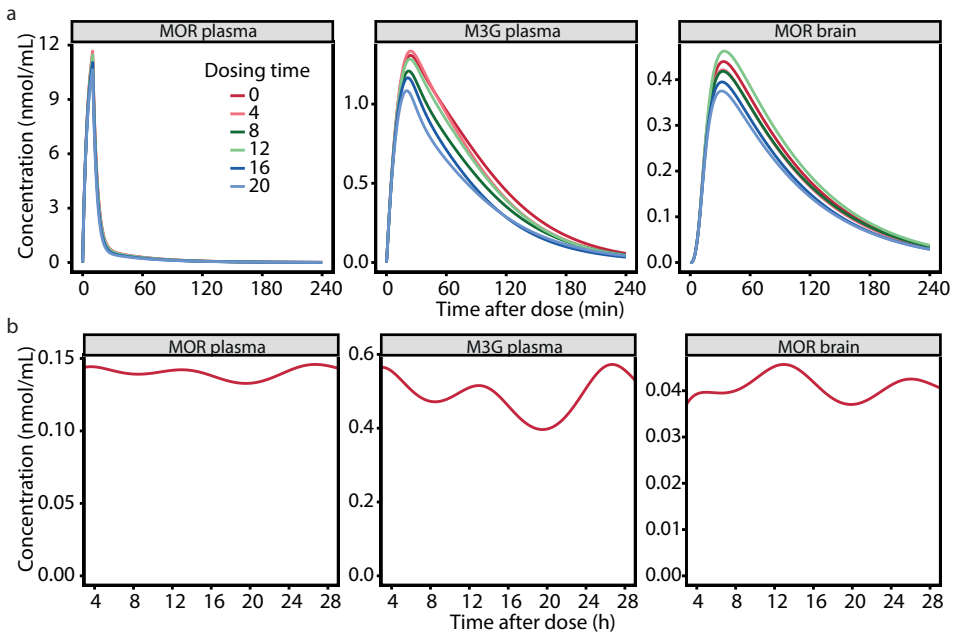

Figure 7 Simulations of morphine (MOR) concentration-time profiles in plasma (left), M3G concentrations in plasma (middle) and morphine concentrations in brain (right) after a 10 min. intravenous infusion of 4 mg/kg at six different dosing times (start of infusion at t=0, 4, 8, 12, 16, 20 hours after light onset) **(a)** and during a continuous infusion of 1mg/kg/h started at 0 hours after light onset **(b)**.

Table 2 Parameter estimates of combined plasma and brain model (with 24-hour variation included on $CL_{10,active}$, $CL_{M3G,active}$ and Q_{ECF-PL}) and results from bootstrap analysis (444/500 resamples successful)

Parameter	Units	Equation	θ	Estimate	RSE	Bootstrap median (90% P.I.)
Morphine plasma						
CL_{10}	mL/min	$CL_{10} = \theta_{CL10,passive} + CL_{10,active} * (1-TRT)$	$\theta_{CL10,passive}$	4.97	4.4%	4.98 (4.63 - 5.35)
			θ_{mesor}	8.24	16.7%	8.19 (6.12 – 10.7)
		With $CL_{10,active} = \theta_{mesor} * (1+\theta_{amp,24} * \cos(2\pi * (t - \theta_{phase,24})/1440) + \theta_{amp,12} * \cos(2\pi * (t - \theta_{phase,12})/720))$	$\theta_{amp,24}$	0.123	46.3%	14.5 (5.61 – 25)
			$\theta_{phase,24}$	1070	11.8%	1053 (839 - 1240)
			$\theta_{amp,12}$	0.126	42%	13.3 (5.17 – 22.6)
			$\theta_{phase,12}$	461	8.6%	463 (384 – 547)
V1	mL	$V1=\theta_{V1}$	θ_{V1}	109	16.3%	109 (80.6 - 144)
Q2	mL/min	$Q2 = \theta_{Q2} * \theta_{Q2,INH}^{TRT}$	θ_{Q2}	11.0	8.9%	11.0 (9.25 – 12.4)
			$\theta_{Q2,INH}$	1.52	5%	1.52 (1.40 – 1.67)
V2	mL	$V2=\theta_{V2}$	θ_{V2}	508	4.9%	505 (454 – 537)
M3G plasma						
$V_{m,MET}$	mL/min	$V_{m,MET} = \theta_{VM} * \theta_{VM,INH}^{TRT}$	θ_{VM}	15.4	7.9%	15.5 (13.7 – 17.7)
			$\theta_{VM,INH}$	0.443	11.7%	0.440 (0.358 – 0.539)
$K_{m,MET}$	nmol/mL	$K_{m,MET}=\theta_{KM}$	θ_{KM}	0.325	18.4%	0.327 (0.250 – 0.490)
CL_{M3G}	mL/min	$CL_{M3G} = \theta_{CLM3G,passive} + CL_{M3G,active} * (1-TRT)$	$\theta_{CLM3G,passive}$	2.8	15.4%	2.76 (2.14 – 3.51)
			θ_{Mesor}	6.85	11.3%	6.83 (5.39 – 8.04)
		With $CL_{M3G,active} = \theta_{mesor} * (1+\theta_{amp,24} * \cos(2\pi * (t - \theta_{phase,24})/1440) + \theta_{amp,12} * \cos(2\pi * (t - \theta_{phase,12})/720))$	$\theta_{amp,24}$	See $CL_{10,active}$		
			$\theta_{phase,24}$	See $CL_{10,active}$		
			$\theta_{amp,12}$	See $CL_{10,active}$		
			$\theta_{phase,12}$	See $CL_{10,active}$		
Morphine brain						
V_{DBR}	mL	$V_{DBR} = \theta V_{DBR}$	θ_{VDBR}	1 FIX		
Q_{DBR}	mL/min	$Q_{DBR} = \theta Q_{DBR}$	θ_{QDBR}	0.0184	6.0%	0.0185 (0.0167 – 0.0209)
V_{ECF}	mL	$V_{ECF} = \theta V_{ECF}$	θ_{VECF}	1 FIX		
Q_{ECF-PL}	mL/min		$\theta_{QECFPL,passive}$	0.0256	9.5%	0.0251 (0.0211 - 0.0301)
			$\theta_{QECFPL,active}$	0.0834	12.4%	0.0824 (0.0659 – 0.103)
		$Q_{ECF-PL} = (\theta_{QECFPL,passive} + Q_{ECFPL,active} * (1-TRT)) * (1 + \theta_{amp,24} * \cos(2\pi * (t - \theta_{phase,24})/1440) + \theta_{amp,12} * \cos(2\pi * (t - \theta_{phase,12})/720))$	$\theta_{amp,24}$	0.376	42%	4.33 (1.75 – 6.82)
			$\theta_{phase,24}$	1390	7.4%	1390 (1150 – 1600)
			$\theta_{amp,12}$	0.633	32.2%	6.76 (3.79 – 10.5)
			$\theta_{phase,12}$	1060	3.3%	1060 (990 – 1120)
Q_{PL-ECF}	mL/min	$Q_{PL-ECF} = \theta_{QPLECF}$	θ_{QPLECF}	0.0322	10.5%	0.0316 (0.260 – 0.0386)
Inter-animal variability (CV%)						
$\omega^2 CL_{10}$				17.3		16.8
$\omega^2 V_{m,MET}$				22.2		21.9
$\omega^2 CL_{M3G}$				43.5		42.6
$\omega^2 Q2$				18.7		18.4
$\omega^2 V_{m,MET} \sim \omega^2 CL_{M3G}$ (untransformed)				0.0761		0.0742
Residual unexplained variability (%)						
σ_{PL}				17.0		16.8
σ_{M3G}				14.5		14.4
σ_{DBR}				11.8		11.3

Simulations

The final model was used to perform simulations to show the impact of dosing time on the concentration profiles of morphine and M3G. As shown in Figure 7A, morphine concentrations in plasma after a single intravenous infusion are minimally affected by dosing time. However, morphine concentrations in brain tissue are influenced by dosing time with the lowest concentrations attained after administration at 20 hours after the onset of the light period and the highest concentrations after 12 hours after the onset of the light period. M3G concentrations were lowest and highest after administration at 4 and 20 hours after the onset of the light period, respectively. During a continuous infusion at steady-state, simulations indicate that morphine and M3G concentrations in plasma and morphine concentrations in brain fluctuate during the 24-hour period (Figure 7B).

DISCUSSION

In this study, we have been able to characterize the effect of dosing time on processes that are involved in the distribution, metabolism and excretion of morphine through the development of a population pharmacokinetic model. By inhibiting P-gp and probenecid-sensitive transporters, the active and passive processes involved in the distribution and clearance of morphine could be investigated separately (Bourasset and Scherrmann, 2006; Groenendaal et al., 2007; Letrent et al., 1999; Tunblad et al., 2003; Xie et al., 1999). We show that the transport of morphine from brain tissue back into the circulation shows a characteristic 24-hour rhythm with the lowest efflux during the light-dark phase transitions. The active processes involved in the clearance of morphine and its metabolite M3G from plasma also show 24-hour variation with the peak in the middle of the dark phase. Using simulations, we show that the concentrations profiles of morphine in brain tissue and of M3G in plasma are affected by time of day. These findings indicate that dosing time should be taken into account in the optimization of morphine's dosing regimen.

Our results show that inhibition of active transport processes by probenecid and tariquidar alters both the systemic pharmacokinetics and the brain distribution of morphine. With regard to systemic pharmacokinetics, inhibition of active transport reduced the systemic clearance of morphine, increased its intercompartmental clearance and lowered the maximal conversion rate of morphine to M3G. Because it was previously found that P-gp inhibition does not influence morphine concentrations in plasma (Groenendaal et al., 2007; Letrent et al., 1998, 1999; Xie et al., 1999), while probenecid treatment has been reported to reduce systemic morphine clearance and the formation of M3G in rats (Tunblad et al., 2003), we hypothesize that the systemic effects we observed are due to probenecid treatment. Probenecid inhibits multiple multidrug resistance proteins (mrps) (Dresser et al., 2001) that are expressed not only in the blood-brain barrier (Stieger and Gao, 2015), but also in the kidney and liver (Lee and Kim, 2004; Zelcer et al., 2001, 2005) and thereby affects the renal and hepatic elimination of drugs (Lee and Kim, 2004). Although we cannot exclude the contribution of other processes, we propose that the effect of probenecid on the systemic

pharmacokinetics of morphine is due to inhibition of mrp transporters in kidney and liver.

Active transport inhibition also altered the brain distribution of morphine. Brain concentrations could be best described by a model in which a "deep brain" compartment was linked to the central plasma compartment by an extra-cellular fluid (ECF) compartment. An additional transport component that was absent inhibitor-treated animals was identified on the transport of morphine from the ECF compartment to plasma. This confirms previous findings that morphine is subject to active efflux transport mediated by P-gp and probenecid-sensitive transporters (Bourasset and Scherrmann, 2006; Groenendaal et al., 2007; Letrent et al., 1999; Tunblad et al., 2003; Xie et al., 1999).

Our findings indicate that several processes involved in morphine pharmacokinetics show 24-hour variation. It was previously shown in cancer patients that the maximal concentration (Cmax) and the area under concentration-time profile (AUC) at steady state are higher at 18:00 than at 10:00 and 14:00 after oral administration (Gourlay et al., 1995). In dogs, the AUC and Cmax of oral sustained release morphine were significantly higher after dosing at 7:30 than after dosing at 19:30 (Dohoo, 1997). However, in the present study, we have been able to quantify the relative contribution of the processes involved in the distribution, metabolism and elimination of morphine more precisely through the use of six dosing times and the development of a population pharmacokinetic model. We find that the active component of the systemic clearance of morphine and M3G show 24-hour variation with a difference of 54% between the lowest value and the highest value. A physiological explanation of these findings could be the observation that the expression of various probenecid-sensitive transporters show 24-hour variation in the kidney (Gachon and Firsov, 2011). However, future research to elucidate the underlying mechanisms is warranted.

Furthermore, we find that the transport of morphine from the brain to the blood shows a 12-hour rhythm with the lowest values at the transitions of the light/dark phase. This rhythm could be described by a 24-hour and 12-hour sinusoidal function on this parameter with a difference between the highest and lowest efflux of 20%. Importantly, the inclusion of this function in the model resolved a time-of-day dependent bias observed in the conditionally weighted residuals. In a previous study we found that the efflux of the P-gp substrate quinidine from the brain to plasma is more than two-fold higher during the dark phase compared to the light phase in the presence of functional P-gp transport, but not when P-gp transport is blocked (Kervezee et al., 2014). In the present study, we do not find this P-gp dependent effect for morphine. While quinidine is a selective P-gp substrate, morphine has more complex transport mechanisms across the BBB, which is not only affected by P-gp but also by probenecid-sensitive transporters. The daily variation in P-gp activity may be (partly) counterbalanced by a differentially-phased variation in probenecid-sensitive transporters. Hence, multiple mechanisms likely give rise to the 12-hour rhythm in the transport of morphine from the brain to blood.

We performed simulations of a single intravenous dose and of a continuous infusion regimen to visualize the effect of the daily rhythmicity in morphine pharmacokinetics on the

concentration-time profiles in plasma and brain tissue. Although morphine concentrations in plasma are minimally affected by dosing time, metabolite concentrations in plasma and morphine concentrations in brain tissue do depend on the time of day. This finding has several important implications: it indicates that time of day can be a substantial source of variation in the pharmacokinetics and, possibly, the pharmacodynamics of morphine when it is not properly accounted for, but also that these systematic variations could be exploited to optimize morphine's dosing regimen.

CONFLICT OF INTEREST

The authors declare no conflicts of interest

ACKNOWLEDGEMENTS

The authors would like to thank Ming Liu for her help with the analysis of the samples. This research was supported by the Dutch Technology Foundation STW, which is the applied science division of NWO, and the Technology Programme of the Ministry of Economic Affairs. The funding source had no involvement in the study design; in the collection, analysis and interpretation of data; in the writing of the report; and in the decision to submit the article for publication.

REFERENCES

Beal, S., Sheiner, L.B., Boeckmann, A., and Bauer, R.J. (2009). NONMEM User's Guides (1989-2009), Icon Development Solutions, Ellicott City, MD, USA.

Bickel, U., Schumacher, O.P., Kang, Y.S., and Voigt, K. (1996). Poor permeability of morphine 3-glucuronide and morphine 6-glucuronide through the blood-brain barrier in the rat. J. Pharmacol. Exp. Ther. 278, 107–113.

Bornschein, R.L., Crockett, R.S., and Smith, R.P. (1977). Diurnal variations in the analgesic effectiveness of morphine in mice. Pharmacol. Biochem. Behav. 6, 621–626.

Boström, E., Hammarlund-Udenaes, M., and Simonsson, U.S.H. (2008). Blood-brain barrier transport helps to explain discrepancies in in vivo potency between oxycodone and morphine. Anesthesiology 108, 495–505.

Bourasset, F., and Scherrmann, J.-M. (2006). Carrier-mediated processes at several rat brain interfaces determine the neuropharmacokinetics of morphine and morphine-6-beta-D-glucuronide. Life Sci. 78, 2302–2314.

Bouw, M.R., Gårdmark, M., and Hammarlund-Udenaes, M. (2000). Pharmacokinetic-Pharmacodynamic Modelling of Morphine Transport Across the Blood-Brain Barrier as a Cause of the Antinociceptive Effect Delay in Rats—A Microdialysis Study. Pharm. Res. 17, 1220–1227.

Cui, Y., Sugimoto, K., Araki, N., Sudoh, T., and Fujimura, A. (2005). Chronopharmacology of morphine in mice. Chronobiol. Int. 22, 515–522.

Dallmann, R., Brown, S.A., and Gachon, F. (2014). Chronopharmacology: new insights and therapeutic implications. Annu. Rev. Pharmacol. Toxicol. 54, 339–361.

Dohoo, S. (1997). Steady-state pharmacokinetics of oral sustained-release morphine sulphate in dogs. J. Vet. Pharmacol. Ther. 20, 129–133.

Dresser, M.J., Leabman, M.K., and Giacomini, K.M. (2001). Transporters involved in the elimination of drugs in the kidney: Organic anion transporters and organic cation transporters. J. Pharm. Sci. 90, 397–421.

Gachon, F., and Firsov, D. (2011). The role of circadian timing system on drug metabolism and detoxification. Expert Opin. Drug Metab. Toxicol. 7, 147–158.

Gourlay, G.K., Plummer, J.L., and Cherry, D.A. (1995). Chronopharmacokinetic variability in plasma morphine concentrations following oral doses of morphine solution. Pain 61, 375–381.

De Gregori, S., De Gregori, M., Ranzani, G.N., Allegri, M., Minella, C., and Regazzi, M. (2011). Morphine metabolism, transport and brain disposition. Metab. Brain Dis. 27, 1–5.

Groenendaal, D., Freijer, J., de Mik, D., Bouw, M.R., Danhof, M., and de Lange, E.C.M. (2007). Population pharmacokinetic modelling of non-linear brain distribution of morphine: influence of active saturable influx and P-glycoprotein mediated efflux. Br. J. Pharmacol. 151, 701–712.

Güney, H.Z., Görgün, C.Z., Tunçtan, B., Uludağ, O., Hodoğlugil, U., Abacioğlu, N., and Zengil, H. (1998). Circadian-rhythm-dependent effects of L-NG-nitroarginine methyl ester (L-NAME) on morphine-induced analgesia. Chronobiol. Int. 15, 283–289.

Junker, U., and Wirz, S. (2010). Review article: chronobiology: influence of circadian rhythms on the therapy of severe pain. J. Oncol. Pharm. Pract. 16, 81–87.

Kavaliers, M., and Hirst, M. (1983). Daily rhythms of analgesia in mice: effects of age and photoperiod. Brain Res. 279, 387–393.

Keizer, R.J., Karlsson, M.O., and Hooker, A. (2013). Modeling and Simulation Workbench for NONMEM: Tutorial on Pirana, PsN, and Xpose. CPT Pharmacometrics Syst. Pharmacol. 2, e50.

Keizer, R.J., Jansen, R.S., Rosing, H., Thijssen, B., Beijnen, J.H., Schellens, J.H.M., and Huitema, A.D.R. (2015). Incorporation of concentration data below the limit of quantification in population pharmacokinetic analyses. Pharmacol. Res. Perspect. 3, e00131.

Kervezee, L., Hartman, R., van den Berg, D.-J., Shimizu, S., Emoto-Yamamoto, Y., Meijer, J.H., and de Lange, E.C.M. (2014). Diurnal Variation in P-glycoprotein-Mediated Transport and Cerebrospinal Fluid Turnover in the Brain. AAPS J. 16, 1029–1037.

Lee, W., and Kim, R.B. (2004). Transporters and renal drug elimination. Annu. Rev. Pharmacol. Toxicol.

44, 137–166.

Letrent, S.P., Pollack, G.M., Brouwer, K.R., and Brouwer, K.L.R. (1998). Effect of GF120918, a Potent P-glycoprotein Inhibitor, on Morphine Pharmacokinetics and Pharmacodynamics in the Rat. Pharm. Res. 15, 599–605.

Letrent, S.P., Pollack, G.M., Brouwer, K.R., and Brouwer, K.L.R. (1999). Effects of a Potent and Specific P-Glycoprotein Inhibitor on the Blood-Brain Barrier Distribution and Antinociceptive Effect of Morphine in the Rat. Drug Metab. Dispos. 27, 827–834.

Lutsch, E.F., and Morris, R.W. (1971). Light reversal of a morphine-induced analgesia susceptibility rhythm in mice. Experientia 27, 420–421.

Morris, R.W., and Lutsch, E.F. (1967). Susceptibility to morphine-induced analgesia in mice. Nature 216, 494–495.

Mould, D.R., and Upton, R.N. (2013). Basic concepts in population modeling, simulation, and model-based drug development-part 2: introduction to pharmacokinetic modeling methods. CPT Pharmacometrics Syst. Pharmacol. 2, e38.

Oliverio, A., Castellano, C., and Puglisi-Allegra, S. (1982). Opiate analgesia: Evidence for circadian rhythms in mice. Brain Res. 249, 265–270.

Potts, A.L., Cheeseman, J.F., and Warman, G.R. (2011). Circadian rhythms and their development in children: implications for pharmacokinetics and pharmacodynamics in anesthesia. Paediatr. Anaesth. 21, 238–246.

Rasmussen, N.A., and Farr, L.A. (2003). Effects of Morphine and Time of Day on Pain and Beta-Endorphin. Biol. Res. Nurs. 5, 105–116.

Somogyi, A. a, Barratt, D.T., and Coller, J.K. (2007). Pharmacogenetics of opioids. Clin. Pharmacol. Ther. 81, 429–444.

Stain-Texier, F., Boschi, G., Sandouk, P., and Scherrmann, J.M. (1999). Elevated concentrations of morphine 6-beta-D-glucuronide in brain extracellular fluid despite low blood-brain barrier permeability. Br. J. Pharmacol. 128, 917–924.

Stieger, B., and Gao, B. (2015). Drug Transporters in the Central Nervous System. Clin. Pharmacokinet. 54, 225–242.

Sverrisdóttir, E., Lund, T.M., Olesen, A.E., Drewes, A.M., Christrup, L.L., and Kreilgaard, M. (2015). A review of morphine and morphine-6-glucuronide's pharmacokinetic-pharmacodynamic relationships in experimental and clinical pain. Eur. J. Pharm. Sci. 74, 45–62.

Thompson, S.J., Koszdin, K., and Bernards, C.M. (2000). Opiate-induced analgesia is increased and prolonged in mice lacking P-glycoprotein. Anesthesiology 92, 1392–1399.

Tunblad, K., Jonsson, E.N., and Hammarlund-Udenaes, M. (2003). Morphine Blood-Brain Barrier Transport Is Influenced by Probenecid Co-Administration. Pharm. Res. 20, 618–623.

Tunblad, K., Hammarlund-Udenaes, M., and Jonsson, E.N. (2004). An Integrated Model for the Analysis of Pharmacokinetic Data from Microdialysis Experiments. Pharm. Res. 21, 1698–1707.

Westerhout, J., Ploeger, B., Smeets, J., Danhof, M., and de Lange, E.C.M. (2012). Physiologically based pharmacokinetic modeling to investigate regional brain distribution kinetics in rats. AAPS J. 14, 543–553.

Xie, R., Hammarlund-Udenaes, M., de Boer, A.G., and de Lange, E.C. (1999). The role of P-glycoprotein in blood-brain barrier transport of morphine: transcortical microdialysis studies in mdr1a (-/-) and mdr1a (+/+) mice. Br. J. Pharmacol. 128, 563–568.

Yoshida, M., Ohdo, S., Takane, H., Tomiyoshi, Y., Matsuo, A., Yukawa, E., and Higuchi, S. (2003). Chronopharmacology of analgesic effect and its tolerance induced by morphine in mice. J. Pharmacol. Exp. Ther. 305, 1200–1205.

Yoshida, M., Koyanagi, S., Matsuo, A., Fujioka, T., To, H., Higuchi, S., and Ohdo, S. (2005). Glucocorticoid hormone regulates the circadian coordination of micro-opioid receptor expression in mouse brainstem. J. Pharmacol. Exp. Ther. 315, 1119–1124.

Zelcer, N., Saeki, T., Reid, G., Beijnen, J.H., and Borst, P. (2001). Characterization of drug transport by the human multidrug resistance protein 3 (ABCC3). J. Biol. Chem. 276, 46400–46407.

Zelcer, N., van de Wetering, K., Hillebrand, M., Sarton, E., Kuil, A., Wielinga, P.R., Tephly, T., Dahan, A., Beijnen, J.H., and Borst, P. (2005). Mice lacking multidrug resistance protein 3 show altered morphine pharmacokinetics and morphine-6-glucuronide antinociception. Proc. Natl. Acad. Sci. U. S. A. 102, 7274–7279.

Zhang, Y.-K.J., Yeager, R.L., and Klaassen, C.D. (2009). Circadian expression profiles of drug-processing genes and transcription factors in mouse liver. Drug Metab. Dispos. 37, 106–115.

Supplementary Table 1 Parameter estimates of combined plasma and brain model (without 24-hour variation included on $CL_{10,active}$, $CL_{M3G,active}$ and Q_{ECF-PL})

Parameter	Units	Equation	θ	Estimate	RSE
Morphine plasma					
CL_{10}	mL/min	$CL_{10} = \theta_{CL10,passive} + \theta_{CL10,active} * (1-TRT)$	$\theta_{CL10,passive}$	4.95	4.5%
			$\theta_{CL10,active}$	8.27	17%
V1	mL	$V1 = \theta_{V1}$	θ_{V1}	110	16.6%
Q2	mL/min	$Q2 = \theta_{Q2} * \theta_{Q2,INH}^{TRT}$	θ_{Q2}	11	8.7%
			$\theta_{Q2,INH}$	1.53	5%
V2	mL	$V2 = \theta_{V2}$	θ_{V2}	511	4.8%
M3G plasma					
$V_{m,MET}$	mL/min	$V_{m,MET} = \theta_{VM} * \theta_{VM,INH}^{TRT}$	θ_{VM}	15.6	7.8%
			$\theta_{VM,INH}$	0.443	11.9%
$K_{m,MET}$	nmol/mL	$K_{m,MET} = \theta_{KM}$	θ_{KM}	0.329	19.1%
CL_{M3G}	mL/min	$CL_{M3G} = \theta_{CLM3G,passive} + \theta_{CL3MG,active} * (1-TRT)$	$\theta_{CLM3G,passive}$	2.82	15.6%
			$\theta_{CLM3G,active}$	6.9	11.4%
Morphine brain					
V_{DBR}	mL	$V_{DBR} = \theta_{VDBR}$	θ_{VDBR}	1 FIX	
Q_{DBR}	mL/min	$Q_{DBR} = \theta_{QDBR}$	θ_{QDBR}	0.0183	6.7%
V_{ECF}	mL	$V_{ECF} = \theta_{VECF}$	θ_{VECF}	1 FIX	
Q_{ECF-PL}	mL/min	$Q_{ECF-PL} = \theta_{QECFPL,passive} + Q_{ECFPL,active} * (1-TRT)$	$\theta_{QECFPL,passive}$	0.0257	9.8%
			$\theta_{QECFPL,active}$	0.0839	13.2%
Q_{PL-ECF}	mL/min	$Q_{PL-ECF} = \theta_{QPLECF}$	θ_{QPLECF}	0.0325	10.6%
Inter-animal variability (CV%)					
$\omega^2 CL_{10}$				18.3	
$\omega^2 V_{m,MET}$				21.7	
$\omega^2 CL_{M3G}$				43.9	
ω^2 Q2				18.3	
$\omega^2 V_{m,MET} \sim \omega^2 CL_{M3G}$				84.0	
Residual unexplained variability (%)					
σ_{PL}				17.4	
σ_{M3G}				14.6	
σ_{DBR}				13.1	

RSE: relative standard error